



**HAL**  
open science

## **CHAPTER 8. Sustainable Activation of Chemical Substrates Under Sonochemical Conditions**

Micheline Draye, Marion L. Chevallier, Vanille Quinty, Claire Besnard, Alexandre Vandepoosele, Gregory Chatel

► **To cite this version:**

Micheline Draye, Marion L. Chevallier, Vanille Quinty, Claire Besnard, Alexandre Vandepoosele, et al.. CHAPTER 8. Sustainable Activation of Chemical Substrates Under Sonochemical Conditions. Sustainable Organic Synthesis: Tools and Strategies, Royal Society of Chemistry, pp.212-238, 2021, Sustainable Organic Synthesis: Tools and Strategies, <10.1039/9781839164842-00212>. <hal-03546738>

**HAL Id: hal-03546738**

**<https://hal.science/hal-03546738v1>**

Submitted on 28 Jan 2022

**HAL** is a multi-disciplinary open access archive for the deposit and dissemination of scientific research documents, whether they are published or not. The documents may come from teaching and research institutions in France or abroad, or from public or private research centers.

L'archive ouverte pluridisciplinaire **HAL**, est destinée au dépôt et à la diffusion de documents scientifiques de niveau recherche, publiés ou non, émanant des établissements d'enseignement et de recherche français ou étrangers, des laboratoires publics ou privés.



HAL Authorization

1 **X. Sustainable Activation of Chemical Substrates Under Sonochemical**

2 **Conditions**

3

4

5

6

7

8 M. Draye, M. Chevallier,<sup>a</sup> V. Quinty,<sup>a</sup> C. Besnard,<sup>a</sup> A. Vandeponseele<sup>a</sup> and G.

9 Chatel<sup>a\*</sup>.

10 <sup>a</sup> Univ. Savoie Mont Blanc, CNRS, EDYTEM, 73000 Chambéry, France.

11 \*corresponding email address: [gregory.chatel@univ-smb.fr](mailto:gregory.chatel@univ-smb.fr)

12

13 **ABSTRACT**

14 Ultrasound activation has been widely explored in organic chemistry to improve the  
15 yields of reaction or their kinetics. The sonochemical approach can also allow  
16 changing the selectivities or limiting the use of hazardous solvents or the amount of  
17 catalyst, in accordance with the principle of green chemistry. However, a rigorous  
18 control of the sonochemical parameters is necessary to better understand the  
19 mechanisms involved under ultrasonic activation.

20

## 21 **X. 1. Introduction**

22 Sonochemistry is the use of power ultrasound for chemical reactions. Some  
23 chemists reported the first reaction involving ultrasound in 1927,<sup>1,2</sup> although the term  
24 “sonochemistry” has only been used since 1980.<sup>3</sup> Ultrasound is often viewed, and  
25 particularly in organic chemistry, as a simple and efficient mixing tool in the lab.  
26 However, a control of the sonochemical parameters and experimental conditions  
27 have made it possible to demonstrate, in many cases, significant improvements in  
28 terms of reaction yields and/or reaction speed, thanks to the use of ultrasound. In  
29 some cases, unexpected reactivities and selectivities have also been observed  
30 under ultrasound, making it possible to imagine new perspectives and applications of  
31 sonochemistry in organic chemistry. After having introduced sonochemistry by  
32 presenting its basic theoretical and practical aspects, some case studies from recent  
33 literature are summarized to show the major advantages of using ultrasound in an  
34 organic reaction. At last, this chapter aims to highlight the current and future  
35 challenges of organic sonochemistry.

## 36 **X. 2. Sonochemistry, a chemistry based on power ultrasound**

### 37 **X. 2. 1. Acoustic cavitation and associated effects**

38 Acoustic cavitation in liquid media is the phenomenon of formation, growth and  
39 violent collapse induced by sound waves that generate fluctuation of pressure. Liquid  
40 media usually contains free gas bubbles or gas molecules trapped in solid impurities,  
41 which can act as nuclei for cavitation<sup>4</sup>. Once the cavitation bubble is formed, its  
42 diameter increases throughout the expansion and compression phases to achieve a  
43 critical size at which it violently collapses. Indeed, expansion phases being isotherm  
44 and compression phases adiabatic, a large amount of acoustic energy is

45 accumulated inside the bubble. At the moment of bubble implosion, temperatures of  
46 about 5,000 K and pressures close to 1,000 bar are then reached within the bubble  
47 (see Figure X.1). These extremes conditions lead to different local effects such as  
48 radicals' formation, shock waves, acoustic micro-currents and violent liquid microjets,  
49 which are at the origin of application of sonochemistry<sup>5,6</sup>.

50 [Insert Figure X.1 here]

51

## 52 **X. 2. 2. Ultrasonic parameters and experimental factors affecting cavitation**

53 The ambient conditions of a reaction system can strongly influence acoustic  
54 cavitation threshold and its intensity, which then directly affects the kinetic and/or the  
55 yield of the chemical reaction. The acoustic cavitation in the liquid may be affected  
56 by several parameters such as the frequency and power of the ultrasounds, the  
57 hydrostatic and external pressures, the temperature, the nature of the solvent and  
58 dissolved gas.

### 59 ***X. 2. 2. 1. Ultrasonic frequency***

60 Ultrasound is a sound wave with a frequency ( $f$ , Eq. X.1) greater than the upper limit  
61 of human hearing, which is generally over 20 kHz and below 10 MHz. When it  
62 propagates in an elastic medium it presents all the general properties of periodic  
63 progressive waves such as propagation, attenuation and reflection<sup>7</sup>.

64 [Insert Equation X.1 here]

65 In water low frequencies, ranging between 20 and 80 kHz, lead to relatively few  
66 and large transient cavitation bubbles; Physical effects such as micromixing, erosion,  
67 etc. predominate over chemical effects. High frequencies, ranging between 150 and

68 2,000 kHz, produce many small transient cavitation bubbles; Chemical effects such  
69 as production of hydroxyl radicals in water predominate over physical effects. It is  
70 noteworthy that, when the frequency increases, the depth of penetration of the  
71 ultrasonic wave decreases, decreasing the maximum pressure reached during  
72 implosion. It is therefore necessary to increase the sound power to obtain the same  
73 effects as at low frequency<sup>7,8</sup>.

#### 74 **X. 2. 2 .2. Dissipated ultrasonic power**

75 A piezoelectric transducer converts electrical energy into mechanical energy that is  
76 thus transmitted to the liquid, which is irradiated<sup>9</sup>. No transducer is 100% efficient in  
77 converting electrical to mechanical power. To determine the power output ( $P_{out}$ ) for a  
78 given power input ( $P_{in}$ ), it is necessary to know the transducer efficiency ( $\eta$ ),  
79 according to Eq. X.2.

80 [Insert Equation X.2 here]

81 The mechanical energy is then converted into acoustical energy generating  
82 acoustic cavitation if the minimum power required is reached, *i.e.*, at the Blake  
83 threshold, which is  $0.5 \text{ W.cm}^{-2}$  at 20 kHz in pure water and at atmospheric pressure<sup>7</sup>.  
84 It is relatively easy to measure the electrical energy delivered by a transducer, but  
85 this value in no way reflects the acoustic energy absorbed by the medium, which is  
86 the only that can be active. Different methods are proposed for the determination of  
87 ultrasonic power ( $P_{acous}$ ) such as thermoacoustic sensor<sup>10</sup>, acousto-optic  
88 interaction<sup>11</sup>, piezoelectric hydrophone<sup>12</sup>, sonoluminescence, and chemical  
89 dosimetry<sup>8</sup>. Nevertheless, one of the most useful methods has been found to be the  
90 calorimetric one<sup>8,13</sup>. Therefore, the absorbed acoustic power  $P_{acous}$  in  $\text{W.mL}^{-1}$ ,  
91 transmitted to the solution can be measured using a conventional thermal probe

92 method<sup>14,15</sup>. Using this method, all energy delivered to the system is considered as  
93 dissipated as heat (Eq. 3).

94 [Insert Equation X.3 here]

### 95 **X. 2. 2. 3. Hydrostatic Pressure**

96 Hydrostatic pressure is a crucial parameter as the conditions within a collapsing  
97 cavitation bubble become more extreme as it increases<sup>16</sup>. Thus, it has been shown  
98 that, cavitation threshold in ultrapure water increases linearly with the hydrostatic  
99 pressure as well as intensity of bubble collapse<sup>8</sup>. Thereby, an optimal hydrostatic  
100 pressure is required to increase the efficiency of ultrasound when used in  
101 sonochemical processes<sup>17</sup>.

### 102 **X. 2. 1. 4. Temperature**

103 When increasing temperature of a liquid, the solubility of gases it contains decreases  
104 whereas its vapor pressure increases decreasing the cavitation efficiency<sup>18</sup>. The  
105 influence of temperature on cavitation threshold is especially noticeable at elevated  
106 hydrostatic pressures and for fluids with large amounts of dissolved gases<sup>19</sup>.

### 107 **X. 2. 1. 5. Nature of the solvent**

108 Properties such as (1) solvent viscosity, (2) its vapor pressure, and (3) its surface  
109 tension can impact ultrasound intensity. For pure solvents the most determining  
110 parameter is the vapor pressure, which when high, decreases cavitation effects<sup>8</sup>.  
111 Thus, combination of a high surface tension with a low viscosity and a low vapor  
112 pressure favors cavitation<sup>18</sup>.

### 113 **X. 2. 1. 6. Dissolved gas**

114 After few acoustic cycles, transient bubbles violently collapse into smaller tiny  
115 bubbles that act as nuclei of new bubbles and create a hot spot with temperatures of  
116 up to 10,000 K<sup>19</sup>. This adiabatic collapse of the bubbles is assumed to allow the  
117 calculation of the temperature and the pressure inside the bubbles according the  
118 equations X4 and X5<sup>20</sup>. Whereas Eq. X.6 allows the calculation of pressure inside  
119 the bubble at the moment of the collapse.

120 [Insert Equations X.4, X.5 and X.6 here]

121 Thus, according to equations X.4 and X.5, a monatomic gas leads to higher  
122 maximum temperatures and pressures and thereby to more violent collapse of the  
123 bubble than a polyatomic gas because its  $\gamma$  value is greater. Thermal effects  
124 consecutive to the collapse of the bubble mainly depend on gas phase thermal  
125 properties such as heat capacity and thermal conduction.

126 In the presence of gas with high thermal conduction, the temperature reached  
127 at the time of implosion is lower than in the presence of a gas with low thermal  
128 conduction, decreasing thus  $T_{max}$ . In addition, increasing the gas content, *i.e.* the  
129 number of gas nuclei of a liquid, leads to lowering of both the cavitation threshold  
130 and the intensity of the shock wave released on the collapse of the bubble.

### 131 **X. 2. 2. 7. External pressure**

132 An increase of  $P_h$  leads to an increase of  $P_m$ , which is the pressure of the medium  
133 (Eq. X.6). In equations X.4 and X.5, when  $P_m$  increases  $T_m$  and  $P_m$  increase, leading  
134 to an increase in the cavitation threshold and the intensity of cavity collapse.

### 135 **X. 2. 2. 8. Ultrasonic intensity**

136 The ultrasonic intensity,  $I_{max}$ , can be expressed as Eq. X.7<sup>7</sup>:

137 [Insert Equations X.7 here]

138 If considering  $\rho$  and  $c$  constant in the medium where the sound propagates,  
139 then  $I_{\max}$  is proportional to the square of the acoustic amplitude  $P_A$ . Thus, an  
140 increase in  $P_A$  leads to an increase of the ultrasonic intensity, which increases the  
141 sonochemical effects up to an optimal value. Indeed, an increase of  $P_A$ , leads to a  
142 decrease of the time available for the collapse of the too large bubble formed that  
143 may become thus insufficient.

144 Likewise, during their propagation through a medium, the intensity of ultrasound  
145 waves decreases when their distance from the emitting source increases (Eq. X.8).  
146 Indeed, sound is attenuated in a liquid medium due to reflection, refraction,  
147 diffraction and/or scattering of the waves, or the conversion of some of their  
148 mechanical energy into heat.

149 [Insert Equation X.8 here]

150 In addition, if too many bubbles are produced at the transducer/liquid interface,  
151 the ultrasonic energy entering the system is attenuated, decreasing the efficiency by  
152 decoupling of the system.

### 153 **X. 2. 3. Mode of irradiation and sonoreactors**

#### 154 **X. 2. 3. 1. Modes of irradiation**

155 Two physic phenomena are widely used to generate ultrasonic waves from  
156 ultrasonic devices: magnetostriction and piezoelectricity. Phenomenon of  
157 magnetostriction takes place when ferromagnetic materials transform an oscillating  
158 magnetic field into mechanical vibration<sup>7</sup>. Piezoelectric effect is the ability of certain  
159 crystalline materials when subjected to an electric field to convert electrical energy

160 into mechanical energy. The strain is then proportional to the applied field and the  
161 mechanical vibrations may lead to ultrasonic sound<sup>21</sup>. This phenomenon is the most  
162 widely used in ultrasound devices.

163 The main materials used are barium titanate ( $\text{BaTiO}_3$ ), synthetic crystals of  
164 lithium niobate ( $\text{LiNbO}_4$ ) and lead zirconate titanate ( $\text{PbTiZrO}_3$ ). These materials are  
165 separated from the reactor by metal or glass and ultrasound waves irradiate directly  
166 or indirectly the reaction medium (see Figure X.2). An immersed titanium probe is  
167 often used as a waveguide.

168 [Insert Figure X.2 here]

### 169 **X. 2. 3. 2. Equipment**

170 Three major sonoreactors are used at lab: ultrasonic bath, cup horn and probe  
171 (Figures X.2, and X.3)<sup>22,23,24</sup>.

172 [Insert Figure X.3 here]

173 Ultrasonic bath, which represents the most common source of ultrasound in  
174 laboratories, is widely used for its low cost. With a frequency of 20 to 60 kHz and  
175 acoustic intensities of 1 to 5  $\text{W}\cdot\text{cm}^{-2}$ , this device is not well adapted to organic  
176 reactions due to the non-homogeneous dissipation of ultrasound energy and the  
177 associated lack of reproducibility of the experiments<sup>25</sup>.

178 Cup-horn reactors present high intensity, which is generally 50 times more  
179 intense than in US baths, and directly irradiate the liquid medium<sup>26</sup>. Their geometry  
180 allows a good distribution of the ultrasonic field. This device is able to produce low  
181 and high frequencies depending of the piezoelectric ceramic chosen and positioned  
182 at the bottom of the reactor for upward irradiation.

183 Ultrasonic probes provide intense ultrasonic energy, which is concentrated at  
184 their tip and approximately 100 times higher compared to ultrasonic baths; they allow  
185 a direct irradiation of the medium.

186 In both cases, the use of a jacketed reactors is recommended to control the  
187 temperature of the medium during the study of organic reactions at lab<sup>6</sup>.

188 In addition, a study of the shape of the reactor may be relevant to avoid dead  
189 zones or to optimize certain physical, thermal and / or chemical effects. Thus, the  
190 tubular reactors, providing radial irradiations, make it possible to focus the high-  
191 intensity ultrasonic field in the heart of the tube and to develop continuous  
192 processes.<sup>27</sup>.

193

### 194 ***X. 2. 3. 3. Characterization of the ultrasonic parameters***

195 A rigorous characterization of sonochemical parameters is crucial to facilitate the  
196 comparison between each study reported in the literature and to understand the  
197 involved mechanisms<sup>6</sup>. Indeed, the used frequency, electric and acoustic powers,  
198 ultrasonic intensity, radical production, shape and geometry of the reactor and other  
199 experimental conditions (temperature, pressure, gas atmosphere, nature and volume  
200 of solvent, etc.) have to be rigorously reported in the experimental part of scientific  
201 publications.

202 The frequency, inherent to the equipment used, is the first parameter to report  
203 to identify which range is used between low frequency (20-80 kHz) and high  
204 frequency (200-2,000 kHz). The electric power also called “nominal electric power”  
205 or “electric power input” is the energy delivered by the device, measured by a  
206 wattmeter (in W). The absorbed acoustical power ( $P_{\text{acous}}$ , expressed in W or  $\text{W}\cdot\text{mL}^{-1}$ )  
207 can be estimated through a calorimetric method using Equation X.3. Acoustic

208 intensity ( $I_{\text{acous}}$ ) is defined as the acoustic power per unit area of the probe (Equation  
209 X.9,  $\text{W.cm}^{-2}$ ).

210 [Insert Equation X.9 here]

211 As previously mentioned, the extreme conditions during the collapse of bubbles  
212 lead to radical production. For example, the sonolysis of water (Scheme X.1) and the  
213 recombination of radical species into hydrogen peroxide (Scheme X.2) are observed  
214 under ultrasonic conditions.

215 [Insert Schemes X.1 and X.2 here]

216 The radical species production can be experimentally estimated or measured  
217 by dosimetry methods<sup>28,29</sup>, Electron Paramagnetic Resonance (EPR),<sup>30</sup> spin-trapping  
218 and/or sonochemiluminescence experiments<sup>31,32,33</sup>. Chemical dosimetry is the most  
219 convenient and employed method. For example, KI dosimetry involves the oxidation  
220 of iodide ions into iodine by hydroxyl radicals formed under ultrasound, through the  
221 reaction shown in Scheme X.3. The concentration of  $\text{I}_3^-$  can be easily measured  
222 using UV-Visible spectrophotometry at a wavelength of 355 nm ( $\epsilon_{\lambda} = 26,303 \text{ L.mol}^{-1}$   
223  $\text{.cm}^{-1}$ ) to deduce the concentration of  $\text{HO}^{\bullet}$  radicals.

224 [Insert Scheme X.3 here]

225 Other methods are used such as Fricke dosimetry (oxidation of  $\text{Fe}^{2+}$  to  $\text{Fe}^{3+}$ ),  
226 terephthalate dosimetry (use of terephthalic acid in alkaline solution) or nitrite and  
227 nitrate dosimetry<sup>6</sup>. The Sonochemical Efficiency (SE) can be defined combining  
228 electric/acoustic power and rate of radicals formation determined by dosimetry  
229 (Equation X10). It constitutes an efficient assessment method to compare different  
230 ultrasonic conditions/reactors.

231 [Insert Equation X.10 here]

232 In EPR spin-trapping experiments diamagnetic nitroso or nitron compounds  
233 are used as spin trap for the conversion short-lived radicals into relatively longer  
234 lived nitroxyl radicals that are observable by EPR spectroscopy<sup>30,34</sup>. This accurate  
235 characterization method is limited by the non-availability of the equipment at lab.

236 The sonoluminescence is the emission of photons during the collapse of  
237 bubbles. The activity of radical or excited species formed in the gas phase of the  
238 bubbles during this collapse can be explored using specific detectors by observing  
239 the UV-Visible spectra of the sonoluminescence<sup>35,36</sup>. The use of luminol solution (3-  
240 aminophthalhydrazide) oxidized by HO<sup>•</sup> radical formed in water under sonochemical  
241 activation leads to the formation of 3-aminophthalic acid with electrons in an excited  
242 state. The visible blue light emission ( $\lambda = 430$  nm) due to the de-energization of  
243 these electrons allows the mapping of effective zones in a sonoreactor, through this  
244 chemiluminescence method<sup>36</sup>.

### 245 **X. 3. Organic sonochemistry: beneficial effects and new reactivities**

#### 246 **X. 3. 1. Green organic sonochemistry**

247 The effects of ultrasound during organic reactions have led to serious improvements  
248 in terms of reactivity and performance, often under mild conditions, in accordance  
249 with a green chemistry approach<sup>37</sup>. Sonochemical reactions in water or biphasic  
250 aqueous systems constitute a great potential for further developments.

251 Sonocatalysis often allows using environmentally friendly conditions, and to  
252 decrease reaction times and reach higher yields. In addition, cavitation phenomenon  
253 leads to physical and chemical effects, which consequences are interesting for  
254 catalyst surface cleaning and free reactive radicals production<sup>38,39</sup>. In the most

255 general cases, the combination of ultrasound activation and a catalyst can lead to  
256 synergistic effects, mainly observed through the physical effects of US on solid  
257 catalysts. Indeed, the physical effects generated by cavitation bubble collapse leads  
258 to improved mass transfer that contributes to permanent cleaning of the catalyst's  
259 surface and increases the probability for compounds to meet and react. Shear forces  
260 induced by shock waves and microstreaming provoke the de-agglomeration of  
261 catalyst, the reduction of particle size, which implies an increase in surface area<sup>40</sup>.  
262 For these reason, poisoning of catalyst can be avoided, the active surface of catalyst  
263 is increased, which leads to higher reaction rates, improved yields and lower  
264 chemicals consumption; this makes sonocatalysis an effective tool for green  
265 chemistry<sup>41,42,43,44,45</sup>. As an example, the S-alkylation of hetaryl thiols was performed  
266 at room temperature six times faster and led to increased yield under US (74% in 30  
267 min) compared to silent conditions (66% in 3 h)<sup>42</sup>. Another synergistic aspect relies in  
268 the microbubbles present in the crevices of solid catalysts. They constitute nuclei for  
269 cavitation bubble, increasing the number of collapsing events<sup>46</sup>. When bubble  
270 collapse near a solid surface such as a solid catalyst particle or vessel, the inrush of  
271 liquid generates an "asymmetrical collapse" disaggregation of the catalyst but also  
272 the fragmentation of the bubble in smaller bubbles that constitute new nuclei for  
273 more cavitation bubbles and collapsing events<sup>47,48</sup>.

274 In the case of semiconductor catalyst such as TiO<sub>2</sub>, electron/hole pairs can be  
275 generated at its surface through the absorption of energy: (UV-)light in the case of  
276 sonoluminescence from cavitation bubbles, or by heat from the extreme temperature  
277 resulting from the collapse of bubbles<sup>41,49</sup>. These charges (electron and hole)  
278 operate in redox reactions with the solvent to form radical species or directly with  
279 organic compounds of the medium. In sonicated reaction medium, the generation of

280 radical species will favor reaction mechanism implying electron transfer rather than  
281 ionic path<sup>23</sup>. For example, the heterocyclization of 1,2-propanediol with fullerene to  
282 form fullerene-fused dioxane adduct was enabled by the improved mixing of the non-  
283 miscible liquid phases, provided by US and also possibly by secondary radical  
284 reaction in the reaction bulk that would react with the C60 fullerene structure<sup>50</sup>. A  
285 change in mechanism and selectivity was describe by Ando where benzyl bromide  
286 reacted with potassium cyanide and alumina in toluene with a Friedel-Crafts  
287 mechanism to afford *o*- and *p*-benzyltoluene when stirred mechanically at 50 °C.  
288 Under 45 kHz US irradiation, the mechanism switched to a nucleophilic substitution  
289 and lead to the production of benzyl cyanide in 71% yield<sup>51</sup>. Bubbles generated by  
290 acoustic waves in the reaction medium are influenced by the presence of solid  
291 catalyst particles and *vice versa*, justifying the beneficial effect of their combination,  
292 called synergy.

293 Another meaning of sonocatalysis is the activation of a reaction by US, through  
294 physical and chemical effects generated by cavitation activity<sup>23</sup>. In that case, the  
295 origin for the effects observed are separated into two categories: true and false  
296 sonocatalysis, “true” being linked to chemical effects such as the generation of  
297 radicals, and false referring to mechanical effects of US<sup>52</sup>.

## 298 **X. 3. 2. Cases studies in organic sonochemistry**

### 299 **X. 3. 2. 1. Examples of oxidation reactions**

300 Many oxidation reactions such as aldehyde<sup>53</sup> or alcohol<sup>54</sup> oxidations have been  
301 studied under ultrasonic irradiation because their mechanisms pass through a radical  
302 route.

303 The aerobic oxidation of D-glucose into D-glucuronic acid was investigated  
304 under high frequency ultrasound (550 kHz,  $P_{\text{acous}} = 0.36 \text{ W.mL}^{-1}$ ) (see Scheme  
305 X.4)<sup>55</sup>. In absence of oxygen, D-glucose was oxidized into D-gluconic acid as main  
306 product (40% yield), while D-glucose under oxygen bubbling was oxidized into D-  
307 glucuronic acid with excellent yield and selectivity (94% and 98%, respectively). The  
308 presence of oxygen bubbling into reaction media allows to increase production rate  
309 of radicals  $\text{HO}^\bullet$ . In this case, mechanisms involving  $\text{HO}^\bullet$  and  $\text{HOO}^\bullet$  were suspected.

310 [Insert Scheme X.4 here]

311 In a very recent study, the  $\text{H}_2\text{O}_2$ -mediated epoxidation of *cis*-cyclooctene  
312 performed under high frequency ultrasonic irradiation (800 kHz,  $P_{\text{acous}} = 0.58 \text{ W.mL}^{-1}$ )  
313 led to improve results compared to silent conditions and revealed important  
314 mechanistic insights of the studied reaction (see Scheme X.5)<sup>56</sup>. Indeed, while a  
315 maximum yield of 89% and a selectivity of 91% were observed under silent  
316 conditions, better results were obtained (96% yield and 98% selectivity) in 30 min  
317 under high frequency ultrasound induced by a good thermoregulation and mild  
318 mixing brought by the sonoreactor. In addition, the non-radical nature of *cis*-  
319 cyclooctene epoxidation mechanism has been demonstrated.

320 [Insert Scheme X.5 here]

321 At last, the oxidative cleavage of double bond of olefins has been studied under  
322 ultrasonic irradiation (see Scheme X.6)<sup>56</sup>. Simultaneous use of ultrasound and  
323 Aliquat 336<sup>®</sup> as phase transfer catalyst was essential to perform the oxidative  
324 cleavage of olefins without organic solvent and in less than 1 h. At room temperature  
325 and thanks to 20 kHz ultrasound probe, mono- and diacids derived from linear and  
326 cyclic olefins are obtained with good to excellent yields, from 65 to 96%.

327 [Insert Scheme X.6 here]

### 328 X. 3. 2. 2. Examples of reduction reactions

329 Amines are important molecules that are involved in the synthesis of amino acids<sup>57</sup>  
330 or vitamins<sup>58</sup> and many of them exhibit interesting biological activities. Therefore,  
331 they are used as antihistaminics, analgesics, antiglycemics<sup>59</sup>, anesthetic<sup>60</sup>,  
332 decongestant<sup>61</sup>, psychostimulant<sup>62</sup> or antidepressant<sup>63</sup>. Classical preparation of  
333 amine derivatives relies on the reduction of nitro precursors using different methods.  
334 Among them hydrogenation catalyzed by metals, is still the most used in the  
335 petrochemical and pharmaceutical industries<sup>64</sup>. However, these methods are often  
336 associated with a lack of chemoselectivity in the presence of other reducible  
337 functions. In addition, the reaction is exothermic, and involves pressurized hydrogen  
338 and flammable solvents, requiring thus particular precautions in terms of safety<sup>65</sup>.  
339 The research of more selective, safe and environmentally friendly method of  
340 reduction is thus an important issue. It is well known that low frequency ultrasonic  
341 irradiation ( $20 \text{ kHz} < f < 80 \text{ kHz}$ ) may enhance catalyst activity and chemical  
342 reactions' kinetic and selectivity<sup>66</sup>. Thus, in 2000, Basu *et al.* described the reduction  
343 of nitroaromatic compounds to the corresponding amines using a Sm/NH<sub>4</sub>Cl  
344 reducing agent under 10 to 25 min of ultrasonic irradiation (see Table X.1)<sup>67</sup>.

345 [Insert Table X.1 here]

346 In Table X.1, 86% of 6-aminochrysene were obtained from 6-nitrochrysene  
347 (Table X.1, compound **2**) after 10 min of sonication using a Sm/NH<sub>4</sub>Cl reducing  
348 agent in methanol, whereas no reaction was observed under silent conditions. 2-  
349 nitro-9H-fluorene (Table X.1, compound **3**) was reduced to 2-aminofluorene in 10  
350 min under ultrasonic irradiation whereas no transformation was observed when the

351 reducing agent was changed for In/NH<sub>4</sub>Cl or for Fe powder/NH<sub>4</sub>Cl. Under silent  
352 conditions, 10 h under methanol reflux were required to reduce 2-nitro-9H-fluorene  
353 (Table X.1, compound **3**) to the corresponding amine. In addition, the reaction was  
354 shown to be selective towards sensitive functional groups such as bromo (Table X.1,  
355 compound **4**), cyano (Table X.1, compound **5**), ester (Table X.1, compound **6**),  
356 unsaturated bonds (Table X.1, compound **7**) and heterocycles (Table X.1, compound  
357 **8**). Unfortunately, ultrasonic frequency and power are not given, making it impossible  
358 to reproduce the experiments under identical conditions.

359 Hypophosphorous acid and its salts are mild, cheap and powerful reducing  
360 agents commonly used for electrochemical applications<sup>68</sup>. Furthermore, sodium  
361 hypophosphite seems has been registered as a non-hazardous substance for Man  
362 and for the Environment in 2010 by REACH<sup>69</sup>. In that context, with sodium  
363 hypophosphite/hypophosphorous acid as reducing system and Pd/C as catalyst,  
364 Letort *et al.* studied the reduction of nitro compounds to the corresponding amines in  
365 H<sub>2</sub>O/2-MeTHF at 60 °C<sup>70</sup>. The authors studied the reaction in terms of solvent effect,  
366 NaH<sub>2</sub>PO<sub>2</sub>/H<sub>3</sub>PO<sub>2</sub> ratio, temperature, Pd/C catalyst loading, with 2-nitroethylbenzene  
367 as model substrate. The methodology scope was then extended to other aliphatic  
368 nitro compounds (see Table X.2) and the results obtained were compared to those  
369 obtained under ultrasonic irradiation.

370 [Insert Table X.2 here]

371 Under the same conditions and even with 1.25 mol% of Pd/C the reduction of  
372 β-nitrostyrene did not lead to the corresponding unsaturated amines nor to the  
373 saturated one, but to a mixture of 44 % of (*Z*)- and 38 % of (*E*)-2-phenylacetaldehyde  
374 oximes<sup>70</sup>. The reaction was found to be faster under ultrasonic irradiation and  
375 especially in the mixture H<sub>2</sub>O/Me-THF (2:1). Thus, a maximum yield of 92% of 2-

376 phenylethan-1-amine was obtained at 60 °C in only 15 min under ultrasonic  
377 irradiation compared to 90 min required under silent conditions. In water as solvent  
378 90 min were required to obtain 35% of amine under silent conditions whereas almost  
379 the double was obtained under ultrasonic irradiation. In water and under ultrasonic  
380 irradiation, a maximal yield of 90% was obtained in 15 min when the temperature  
381 was increased to 70 °C. The use of a vibromixer allowed the authors to attribute the  
382 effects of ultrasound to the formation of an intense micro-emulsion and classified the  
383 reaction as a type II reaction termed as “false sonochemistry”.

### 384 **X. 3. 2. 3. Examples of fused heterocycles**

385 *N*-containing heterocycles are essential building blocks for the synthesis of many  
386 biologically active compounds<sup>71,72</sup>. In that context, Nongrum *et al.* described the  
387 synthesis of fused benzo *N,N*-containing heterocycles under ultrasonic activation  
388 and using 1-désoxy-1-(méthylamino)-D-glucitol, *i.e.*, meglumine, as organocatalyst<sup>73</sup>.  
389 The authors used meglumine, an environmental water-soluble amino sugar, to  
390 catalyze the reaction in association with ultrasound as alternative activation technic  
391 with mixture ethanol-water as solvent. The reaction was optimized in terms of  
392 catalyst loading, solvent and activation technique with 1,2-phenyldiamine, dimedone  
393 and tolualdehyde as substrates. The scope of the reaction was then extended to  
394 aromatic aldehydes bearing electron-withdrawing and -donating substituents,  
395 leading to excellent yields under 20 to 30 min of ultrasonic irradiation (see Table  
396 X.3)<sup>73</sup>. Two hypotheses have been formulated to explain the role of meglumine,  
397 which is suggested to act via electrophilic or nucleophilic activation of dimedone.  
398 Under the same conditions, 85 to 90% of quinoxaline derivatives were synthesized  
399 under 25 to 35 min of ultrasonic irradiation at 50 °C.

400 [Insert Table X.1 here]

401 Using an acidic ionic liquid, the 1,4-diazabicyclo[2,2,2]octanium diacetate, *i.e.*,  
402 DABCO diacetate, Fekri *et al.* synthesized 93 to 97 % of various benzodiazepines  
403 under 8 to 17 min of ultrasonic irradiation (see Table X.4)<sup>74</sup>. The reaction under silent  
404 conditions and at 90 °C afforded the products in higher reaction times and lower  
405 yields. A mechanism involving the ionic liquid for increasing the electrophilicity of the  
406 carbonyl substrates is then proposed.

407 [Insert Table X.4 here]

### 408 X. 3. 2. 4. Examples of organometallic reactions

409 Sonochemistry is a green alternative method to classical methods to promote the  
410 synthesis of organic compounds, offering then versatile and easy pathways for a  
411 wide variety of transformations such as Reformatsky, Barbier-Grignard or Michael  
412 reactions<sup>75</sup>.

413 The Reformatsky reaction, which converts aldehydes and ketones to  $\beta$ -  
414 hydroxyesters, is one of the first organometallic reactions with problems of metal  
415 activation under silent conditions that was studied under ultrasound. In 1982, it was  
416 shown that the addition of ultrasound resulted in better reaction yields in less time  
417 compared to silent conditions<sup>76</sup>. In fact, for a reaction time of 12 h, the yield was 58%  
418 while with ultrasound (ultrasonic bath, frequency not indicated), it rose to 98% in only  
419 30 min. Several studies were carried out in order to understand the role of ultrasound  
420 in this reaction<sup>77,78,79</sup>. Authors reported successful syntheses with quantitative yields  
421 of  $\beta$ -hydroxyester by reacting phenylketons,  $\alpha$ -bromoesters, zinc dust and a catalytic  
422 amount of iodine under high intensity ultrasonic irradiation<sup>80</sup>. But, the role of iodine  
423 was not fully understood. Reformatsky reactions could then be carried out using non-  
424 traditional electrophiles such as glyoxylic oximes<sup>81</sup>.

425 In the Barbier-Grignard type reaction, the organometallic reagent, which  
426 intervenes, serves as a nucleophile for the formation of a carbon-carbon bond<sup>82</sup>. The  
427 zinc-mediated Barbier reaction was carried out in a biphasic CO<sub>2</sub>/H<sub>2</sub>O system  
428 allowing a preferential partitioning of the desired homoallyl alcoholic product<sup>83</sup>. Here,  
429 pulsed ultrasound is efficient for dispersing and mixing the two phases creating thus  
430 an emulsion while ensuring the kinetic control.

431 The Michael reaction is often a first choice organic transformation because  
432 there are a large number of Michael acceptors and nucleophiles. Indeed, almost all  
433 activated alkenes such as  $\alpha,\beta$ -unsaturated ketones can act as acceptors. It is also  
434 possible in a single step to form stereogenic centers<sup>84</sup>. Numerous studies have  
435 demonstrated the need for basic or acidic catalysts in the reaction of addition of  
436 nucleophiles 1,4-conjugated to unsaturated carbonyl compounds<sup>85</sup>. However, these  
437 conditions gave way to side reactions. The effects of ultrasound then allowed a more  
438 efficient approach when adding the conjugate<sup>86</sup>. In a recent study, researchers  
439 studied the chemical behavior of 3-diethyl phosphonocoumarin in an ultrasound-  
440 assisted Michael-type reaction<sup>87</sup>. Several organometallic compounds have been  
441 selected to react with this coumarin as hard nucleophiles isomers (see Scheme X.7).  
442 This approach allowed the use of a simpler experimental set and milder reaction  
443 conditions. Excellent reproducibility of yield is reported as well as high  
444 diastereoselective activity of isolated *trans* isomers<sup>87</sup>.

445 [Insert Scheme X.7 here]

### 446 X. 3. 3. Scale-up and industrial applications

447 In organic sonochemistry, a series of macroscopic characteristics, namely the use of  
448 less toxic/hazardous chemicals, eco-friendly solvents, alternative or renewable raw

449 materials, the development of reaction conditions to increase the selectivity of the  
450 product or even the minimization of consumption energy during transformations  
451 reinforce the aspect sought in green chemistry and encourage the use of ultrasound  
452 on a larger scale<sup>6,88</sup>.

453 As presented previously, lab scale experiments in organic chemistry are very  
454 promising to create green processes in industry<sup>23,89</sup>. However, to our knowledge, no  
455 industrial scale sonoreactor was successfully employed for organic synthesis. Large  
456 scale transfers require adjustments concerning various parameters and a scale-up  
457 methodology is lacking<sup>90</sup>.

458 The efficiency of sonochemical reactions relies on hydrodynamics, mixing and  
459 mass transfer. Two types of parameters need to be studied when scaling up a lab-  
460 scale experiment to industrial purpose: (i) the operating parameters such as the  
461 frequency, the intensity and the initial radius of bubble nuclei and (ii) the geometric  
462 parameters such as the size and location of transducers, the shape and dimensions  
463 of the reactor. Both types of parameters will impact the mixing and hydrodynamic  
464 characteristics that define the cavitation field. The main problems in intensifying  
465 organic reactions relate to the fact that the yield and selectivity of the chemical  
466 reaction are non-linearly based on operating parameters and geometry; a  
467 proportional amplification of the dimension of the reactor is therefore not sufficient to  
468 reproduce the same experimental conditions. Fine predictions of many parameters  
469 such as pressure, temperature, and cavitation activity distribution are required to  
470 achieve chemical reaction effectiveness. Another problem frequently encountered is  
471 that cavitation events happen mainly near the irradiating surfaces. The adjustment of  
472 lab-scale reaction at large-scale requires higher energy input to counterbalance  
473 energy dissipation in wider bulk media leading to fast erosion of the sonication

474 surfaces<sup>90</sup>. Large-scale reactors contain larger volumes, which bring the issue of US  
475 attenuation, due to reflection, refraction or absorption of the incident sound wave and  
476 leads to spatial variation of the cavitation activity, creating active and passive  
477 zones in the reactor. This needs to be avoided to perform chemical reactions at an  
478 industrial scale<sup>91</sup>.

479 To anticipate the problematics related to large scale sonoreactors, experimental  
480 measurements and theoretical techniques exist to predict the cavitation activity  
481 distribution. The mapping of a sonoreactor can contribute to upscale chemical  
482 reactions. It consists in the characterization of the cavitation phenomena and  
483 implies the quantification of primary effects (generated at the same time as the  
484 bubble collapse) and secondary effects (generated after bubble collapse).  
485 Parameters like pressure can be quantified using a hydrophone while changes in  
486 local temperature can be measured with a thermocouple<sup>92</sup> and gives information on  
487 the local cavitation activity and is used to quantify the efficacy of the sonochemical  
488 reactor in term of energy transfer. The quantification of secondary parameters as  
489 radical production can be assessed through dosimetry. Chemical reaction implying  
490 hydroxyl radicals enable an indirect measure of their concentration and they can  
491 have large measurement errors<sup>93</sup>. The modelling of cavitation parameters such as  
492 pressure, temperature but also the bubble radius and the chemical species formed  
493 can be predicted through modelling<sup>94,95</sup>. Large scale reactors imply specific studies  
494 as for example, the pressure of the reaction medium is a function of depth and  
495 impacts the conditions of cavitation bubble collapse like pressure and temperature,  
496 and thus the physical and chemical effects on chemical reactions<sup>96,97</sup>. Concerning  
497 sonochemical efficiency assessment, most studies are conducted on single bubble

498 model<sup>98,99</sup> which does not take account of neighbor bubbles behavior mutually  
499 influencing the other bubble behavior<sup>100,101</sup>.

500 The scaling-up of organic reaction under US would enable great energy and  
501 chemical savings. The main difficulty to design large scale reactors is to ensure a  
502 uniform distribution of cavitation activity. Empirical methods and theoretical  
503 modelling can be used to work on this aspect and contribute to the industrialization  
504 of US for organic synthesis.

#### 505 **4. Conclusions: from the challenges to new perspectives of organic** 506 **sonochemistry**

507 Since the evaluation of the eco-compatibility of a process cannot be done  
508 subjectively, there are a certain number of calculations of green chemistry such as  
509 the economy of atoms, the mass reaction efficiency, the intensity mass, effective  
510 mass yield, carbon efficiency, the E-factor, the Eco-Scale or other green  
511 metrics<sup>102,103</sup>. These tools are still little exploited by sonochemists and the  
512 systematization of their use is recommended. The systematic comparison between  
513 silent and ultrasonic conditions are necessary, under the same conditions, to  
514 highlight the improvements brought by ultrasound in terms of efficiency and eco-  
515 compatibility. For example, the energy consumption should be also measured. At lab  
516 scale, *in situ* data monitoring can be collected to extrapolated the ultrasound  
517 conditions at a higher scale<sup>104</sup>.

518 In terms of equipment, the combined efforts of chemists, physicists and  
519 equipment manufacturers will be needed for the chemical process industry to exploit  
520 cavitation as a more viable option for chemical transformations.

521 As a perspective, the combination of ultrasound with other physical and  
522 chemical methods of activation seems promising. For example, the use of subcritical  
523 H<sub>2</sub>O (hydrothermal, 200 °C) under ultrasonic irradiation (20 kHz) shows stable  
524 cavitation with nonlinear bubble oscillations. On the other hand, formation of  
525 hydrogen peroxide H<sub>2</sub>O<sub>2</sub> thermally unstable is not observed<sup>105</sup>. Sonohydrothermal  
526 synthesis is described for the synthesis of inorganic nanomaterial<sup>106</sup>, but not yet for  
527 organic synthesis. Indeed, the combination of ultrasound with supercritical CO<sub>2</sub> has  
528 not been used in organic chemistry due to high pressure and lack of phase  
529 boundaries observed in the supercritical state<sup>107</sup>. Hence, for biomass valorization,  
530 positive influence of ultrasound in supercritical CO<sub>2</sub> is observed thanks to  
531 mechanical effects (micro- and macro-mixing, cell damage) that could be useful in  
532 organic synthesis<sup>108</sup>.

533 In organic synthesis, the use of US and microwaves in tandem or  
534 simultaneously at laboratory scale improves selectivity, yield and lowers reaction  
535 times<sup>109,110</sup>, satisfying some principles of green chemistry criteria. The synergistic  
536 effects observed are commonly attributed to the improved heat transfer provided by  
537 microwaves and the intense mass transfer resulting from US. Each irradiation  
538 technology compensates the weakness of the other, which justifies the added value  
539 of their simultaneous use, especially in heterogeneous systems<sup>110,111</sup>.

540 Despite the many advantages of microreactors, one major drawback is the  
541 potential clogging of their channels<sup>112</sup>. In that context, the synergy of ultrasound and  
542 microfluidics has shown its potential. Thus, Sedelmeier *et al.*<sup>113</sup> used an ultrasonic  
543 bath to avoid the fouling of the microreactor due to the deposition of manganese  
544 dioxide used for the oxidation of nitroalkanes into their corresponding carboxylic acids.  
545 Recently, Delacour *et al.*<sup>114</sup> developed a scaled-up ultrasonic reactor to prevent

546 clogging in particle forming reactions. The millireactor was used for the synthesis of  
547 barium sulphate. Results showed that only  $0.48 \text{ W.mL}^{-1}$  was required to prevent  
548 channel clogging and to increase the productivity by two orders of magnitude  
549 compared to a microreactor.

550 Sonophotocatalysis, which is the combination of sonochemistry and  
551 photocatalysis, has mainly been used as an advanced oxidation process for the  
552 removal of pollutants. Its recent use in organic synthesis showed promising results  
553 as a synergistic effect of both activation methods afforded an alkyl carbon chain  
554 elongation from 3 C (malonic acid) to 4 C (succinic acid). The carbon chain  
555 elongation was observed only when US and UV irradiations were combined<sup>115</sup>.

556 At last, the physicochemical properties of some ionic liquids (ILs), such as their  
557 large thermal stability, their wide liquid domain or even their low vapor pressure  
558 make them very interesting reaction media for green chemistry. The combination of  
559 ultrasound with the appropriate ionic liquid is a powerful tool for performing various  
560 organic transformations<sup>116</sup>. The rate of reactions, selectivity and yields are often  
561 improved. Their combination with US then makes it possible to obtain the desired  
562 products without using inorganic or organic catalysts, even at room temperature<sup>117</sup>.  
563 The possible degradation phenomena (few ppm) of ILs under US conditions have  
564 nevertheless to be considered<sup>118</sup>. Deep eutectic solvents are also very promising as  
565 a green alternative in synergy with ultrasound in organic syntheses<sup>119</sup>.

566 When combining processes, technologies, tools or reagents, an interesting way  
567 to assess to efficiency of the coupling is to calculate its synergy. Synergy  
568 corresponds to a beneficial effect from a coupling that is positive if the results  
569 obtained with the coupling of processes is superior to the sum of the results obtained

570 with each independent process<sup>109</sup>. Several indicators of synergy can be found in the  
 571 literature but their definition and the equations that are used should always be  
 572 detailed to avoid confusion. Among indicators for synergy the following can be found:  
 573 synergy, synergy effect, synergistic effect, %synergy or synergy index<sup>120,121,122</sup>. For  
 574 example, the equation for percentage of synergy (Equation X.11) and the synergy  
 575 index (Equation X.12) for n processes leading to chemical reactions with k as rate  
 576 constant, are detailed below.

577 [Insert Equations X.11 and X.12 here]

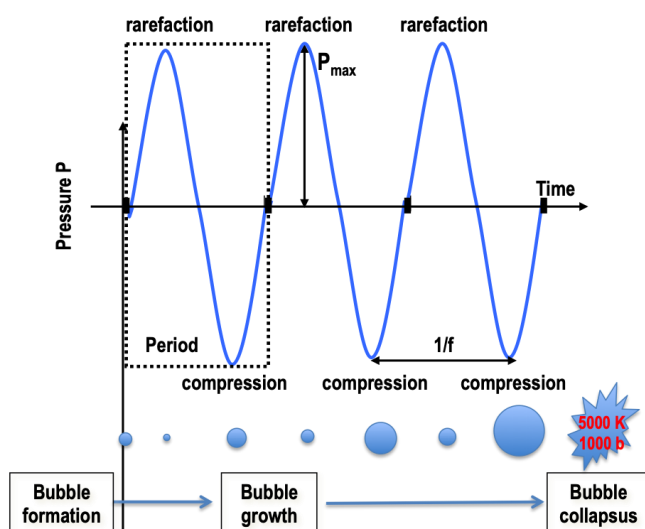
578 The calculation of the %synergy and synergy index are recommended when  
 579 ultrasound are combined in an organic reaction with another physical or chemical  
 580 activation method in order to prove the advantages of the used combination.

581

582

### 583 FIGURE AND TABLE CAPTIONS

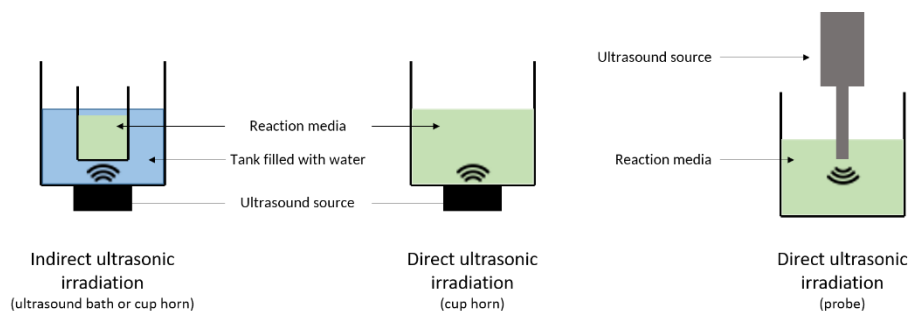
584 **Figure X.1:** Schematic representation of bubble formation, growth and collapsing.



585

586

587 **Figure X.2:** Schematic representation of mode of irradiation depending on the main  
 588 device used in laboratories (adapted from reference <sup>123</sup>).



589  
 590

591 **Figure X.3:** Cup horn system (left) and ultrasonic probe (right) at lab.



592

593 **Table X.1:** Reduction of aromatic nitro compounds by Sm/NH<sub>4</sub>Cl under ultrasonic  
 594 irradiation (ultrasonic bath, frequency not indicated, room temperature)<sup>67</sup>.  
 595

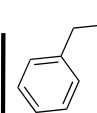
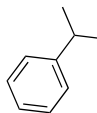
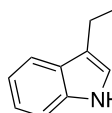
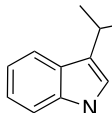
	$\text{Ar-NO}_2 \xrightarrow[\text{MeOH, r.t.}]{\text{Sm/NH}_4\text{Cl (4/20)}} \text{Ar-NH}_2$							
Ar-NO <sub>2</sub>								
	1	2	3	4	5	6	7	8
Time, min	10	10	10	10	10	10	10	25
Yield, %	88	86	92	88	87	74	90	56

596

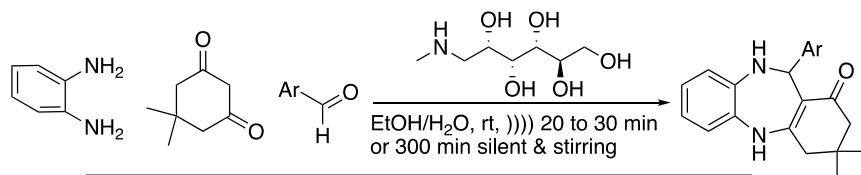
597

598 **Table X.2:** Reduction of aliphatic nitro compounds under silent and ultrasonic  
 599 conditions (ultrasonic microtip, 20 kHz, P<sub>acous</sub> = 3.94 W, 3 mL)<sup>70</sup>.

$$\text{RNO}_2 \xrightarrow[\text{H}_2\text{O}/2\text{-MeTHF (2:1), )}) \text{or silent, 60}^\circ\text{C}]{\text{NaH}_2\text{PO}_2/\text{H}_3\text{PO}_2 (4:1), \text{Pd/C, time}} \text{RNH}_2$$

R				
Activation method	Silent / )))	Silent / )))	Silent / ))) / ))) / ))) / ))) / )))	Silent / ))) / ))) / ))) / ))) / )))
Time, min	90 / 15	90 / 15	90 / 10 / 20 / 30 / 30	90 / 15 / 20 / 30 / 30
Catalyst loading, mol%	0.6 / 0.6	0.6 / 0.6	0.6 / 0.6 / 0.6 / 0.6 / 1.25	0.6 / 0.6 / 0.6 / 0.6 / 1.25
Yield, %	90 / 90	84 / 84	98 / 61 / 78 / 84 / 98	80 / 78 / 80 / 85 / 85

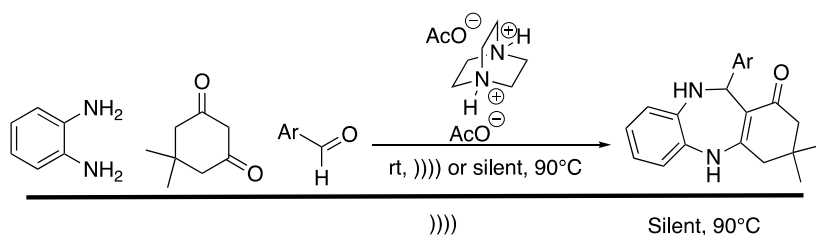
600

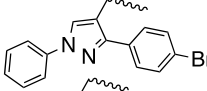
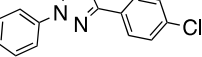
601 **Table X.3:** Synthesis of 1 *H*-dibenzo[*b,e*][1,4]diazepin-1-one derivatives with 5 mol%602 of meglumine as catalyst under silent and ultrasonic conditions (ultrasonic bath)<sup>73</sup>.

Ar	)))		Silent 300 min
	Time, min	Yield, %	Yield, %
C <sub>6</sub> H <sub>5</sub>	20	92	65
4-CH <sub>3</sub> C <sub>6</sub> H <sub>4</sub>	20	92	68
4-OCH <sub>3</sub> C <sub>6</sub> H <sub>4</sub>	20	88	65
4-ClC <sub>6</sub> H <sub>4</sub>	25	90	60
4-BrC <sub>6</sub> H <sub>4</sub>	25	92	68
4-NO <sub>2</sub> C <sub>6</sub> H <sub>4</sub>	30	85	58
4-OHC <sub>6</sub> H <sub>4</sub>	25	88	60
4-N(CH <sub>3</sub> ) <sub>2</sub> C <sub>6</sub> H <sub>4</sub>	30	88	64
2-ClC <sub>6</sub> H <sub>4</sub>	25	82	62
2-NO <sub>2</sub> C <sub>6</sub> H <sub>4</sub>	30	85	55
1-Naphthyl	25	88	55
Furfuryl	30	88	64
C <sub>6</sub> H <sub>5</sub> CH=CH	30	82	60
4-(OH) and 3-(OCH <sub>3</sub> )C <sub>6</sub> H <sub>3</sub>	25	90	65
3,4-(OCH <sub>3</sub> ) <sub>2</sub> C <sub>6</sub> H <sub>3</sub>	20	90	60

603

604 **Table X.4:** Synthesis of various benzodiazepines with 0.5 mmol of ionic liquid as605 catalyst under silent and ultrasonic conditions (ultrasonic bath, 45 kHz, P<sub>in</sub> = 305606 W)<sup>74</sup>.

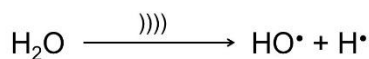


Ar	))))		Silent, 90°C	
	Time, min	Yield, %	Time, min	Yield, %
C <sub>6</sub> H <sub>5</sub>	10	95	75	82
4-ClC <sub>6</sub> H <sub>4</sub>	8	97	60	84
4-OCH <sub>3</sub> C <sub>6</sub> H <sub>4</sub>	8	96	60	85
4-NO <sub>2</sub> C <sub>6</sub> H <sub>4</sub>	8	98	60	89
3-NO <sub>2</sub> C <sub>6</sub> H <sub>4</sub>	10	95	75	88
3-ClC <sub>6</sub> H <sub>4</sub>	10	96	75	89
4-N(CH <sub>3</sub> ) <sub>2</sub> C <sub>6</sub> H <sub>4</sub>	12	93	90	85
2,4-diClC <sub>6</sub> H <sub>4</sub>	15	94	90	83
	6	95	60	82
	17	94	90	81

607

608

609

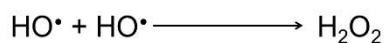
610 **Scheme X.1:**

611

612

613 **Scheme X.2:**

614

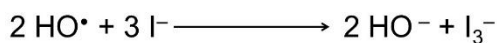


615

616

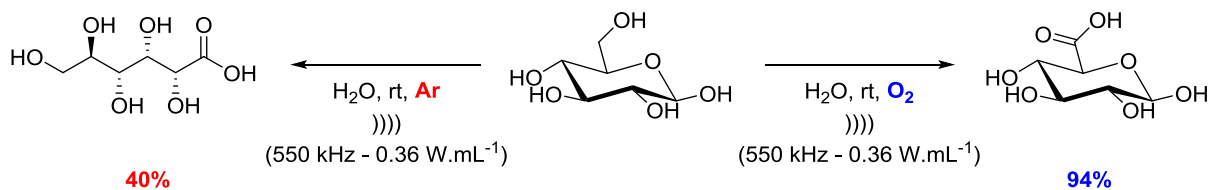
617 **Scheme X.3:**

618



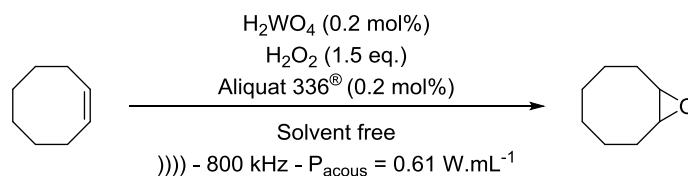
619

620

621 **Scheme X.4:**

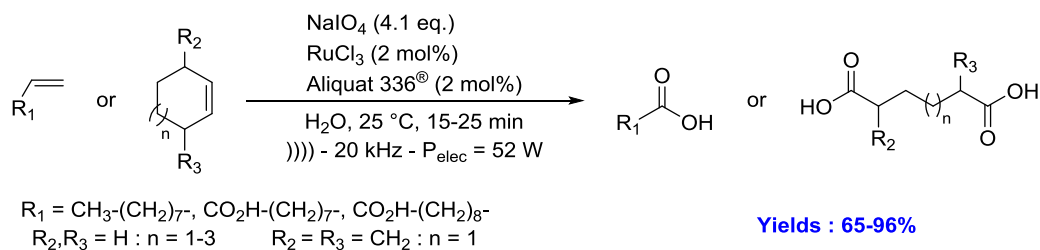
622

623 **Scheme X.5:**



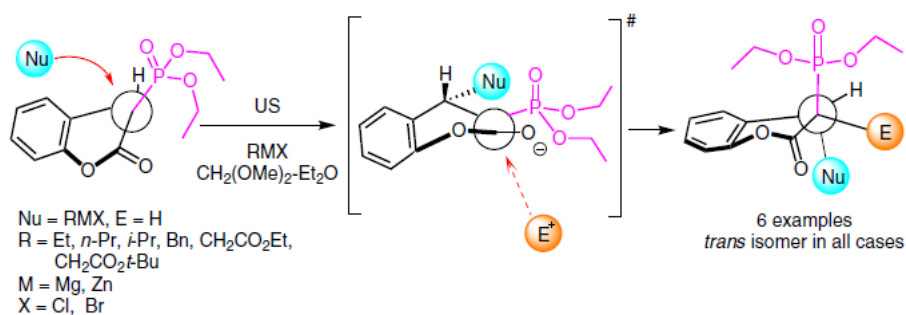
624  
625  
626

**Scheme X.6:**



627  
628

629 **Scheme X.7:**



630

631 **Equation X.1.**

632 
$$f = \frac{c}{\lambda}$$

633 where  $f$  is the frequency (Hz),  $c$  is the celerity of sound ( $\text{m.s}^{-1}$ ) and  $\lambda$  the wavelength (m).

634

635 **Equation X.2.**

636 
$$P_{\text{out}} = h \times P_{\text{in}}$$

637

638 **Equation X.3.**

639 
$$P_{\text{acous}} = m \times c_p \times \left(\frac{dT}{dt}\right)_0$$

640 where  $P_{\text{acous}}$  is the absorbed acoustical power in W (or reported to the volume in  $\text{W}\cdot\text{mL}^{-1}$ ),  $m$   
 641 is the mass in kg of liquid in the sonoreactor,  $c_p$  is the specific heat capacity in  $\text{J}\cdot\text{kg}^{-1}\cdot\text{K}^{-1}$ ,  
 642  $\left(\frac{dT}{dt}\right)_0$  is the initial slope of the increase of the temperature of the solution versus time of  
 643 ultrasonic irradiation.

644

#### 645 **Equations X.4., X.5 and X.6**

$$646 \quad P_{max} = P \left[ \frac{P_m(\gamma-1)}{P} \right]^{\frac{\gamma}{\gamma-1}} \quad \text{Eq. X.4}$$

$$647 \quad T_{max} = T_0 \left[ P_m \frac{(\gamma-1)}{P} \right] \quad \text{Eq. X.5}$$

648

$$649 \quad P_m = P_a + P_h \quad \text{Eq. X.6}$$

650 where  $P_{\text{max}}$  and  $T_{\text{max}}$  are the maximum pressure and temperature at the collapse,  $P$  is the  
 651 pressure inside the bubble at its maximum size; it is usually equal to the vapor pressure  $P_v$ ,  
 652  $P_m$  is the pressure inside the liquid at the moment of the collapse,  $T_0$  is the ambient  
 653 temperature,  $P_a$  is the acoustic pressure applied,  $P_h$  is the pressure within the fluid. It is  
 654 usually taken to be ambient or atmospheric pressure. The polytropic factor  $\gamma$  is the ratio of  
 655 the specific heat capacities of the gas or the gas vapor mixture.

656

#### 657 **Equation X.7.**

$$658 \quad I_{max} = \frac{P_A^2}{2\rho c}$$

659 where  $P_A$  is the acoustic amplitude,  $\rho$  is the density of the medium, and  $c$  is the velocity of  
 660 the sound in the medium.

661

#### 662 **Equation X.8.**

663  $I_{max} = I_0 e^{-2\alpha d}$

664 where  $I_0$  is the initial sound intensity,  $\alpha$  is the absorption coefficient of the medium and  $I_{max}$  is  
 665 the ultrasonic intensity at the distance  $d$ .

666

667 **Equation X.9.**

668

$$I_{acous} = \frac{P_{acous}}{S_{probe}}$$

669 where  $I_{acous}$  is the acoustic intensity ( $W.cm^{-2}$ ),  $P_{acous}$  is the acoustic power (W) and  $S_{probe}$  is  
 670 the surface of the irradiating probe.

671 **Equation X.10.**

$$SE_{elec/acous} = \frac{n_{ions}}{E_{elec/acous}}$$

672 where SE is the Sonochemical Efficiency ( $mol.J^{-1}$ ),  $n_{ions}$  is the number of moles of considered  
 673 produced under ultrasonic irradiation (mol of  $I_3^-$ ,  $NO_2^-$ ,  $NO_3^-$  depending of the dosimetry  
 674 method) and  $E_{elec/acous}$  is the electrical or acoustic power (W, electric or acoustic).

675 **Equation X.11.**

$$\%synergy = 100 \frac{k_{combined\ processes} - \sum_{i=1}^n k_{process\ i}}{k_{combined\ processes}}$$

677 **Equation X.12.**

$$synergy\ index = \frac{k_{combined\ processes}}{\sum_{i=1}^n k_{process\ i}}$$

679

680 **ABBREVIATIONS:**

681 c: celerity of sound

682  $c_p$ : specific heat capacity

- 683 DABCO: 1,4-Diazabicyclo[2.2.2]octane
- 684  $E_{\text{elec/acous}}$ : electrical or acoustic power
- 685 EPR: Electron Paramagnetic Resonance
- 686  $f$ : frequency
- 687  $I_0$ : initial sound intensity
- 688  $I_{\text{acous}}$ : acoustic intensity
- 689  $I_{\text{max}}$ : ultrasonic intensity
- 690 ILs: Ionic Liquids
- 691  $m$ : mass of liquid in the sonoreactor
- 692  $P$ : pressure inside the bubble at its maximum size
- 693  $P_a$  is the acoustic pressure applied
- 694  $P_A$ : acoustic amplitude
- 695  $P_{\text{acous}}$ : acoustical power
- 696  $P_h$ : pressure within the fluid
- 697  $P_{\text{in}}$ : power input
- 698  $P_m$ : pressure inside the liquid at the moment of the collapse
- 699  $P_{\text{max}}$ : maximum pressure at the collapse
- 700  $P_{\text{out}}$ : power output
- 701  $P_v$ : vapor pressure at the moment of the collapse
- 702 REACH: Registration, Evaluation and Authorisation of Chemicals
- 703 SE: Sonochemical Efficiency

- 704  $S_{\text{probe}}$ : surface of the irradiating probe
- 705  $T_0$ : ambient temperature
- 706  $T_{\text{max}}$ : temperature at the collapse
- 707 US: Ultrasound
- 708 UV: Ultraviolet
- 709  $\lambda$ : wavelength
- 710  $\left(\frac{dT}{dt}\right)_0$ : initial slope of the increase of the temperature of the solution versus time of ultrasonic irradiation
- 711 irradiation
- 712  $\alpha$ : absorption coefficient of the medium
- 713  $\gamma$ : polytropic factor
- 714  $\rho$ : density of the medium

715

716 **REFERENCES:**

- 
1. R. Woods and A. Loomis, *Philos. Mag.*, 1927, **4**, 414.
  2. T. Richards and A. Loomis, *J. Amer. Chem. Soc.*, 1927, **49**, 3086.
  3. E. Neppiras, *Phys. Rep.*, 1980, **61**, 159.
  4. S. K. Bhangu and M. Ashokkumar, *Top. Curr. Chem.*, 2016, **374**, 1.
  5. T. Lepoint and F. Lepoint-Mullie, *Theoretical Bases*, In: *Synthetic Organic Sonochemistry*, Plenum Press, 1998, 1-49.

- 
6. G. Chatel, *Sonochemistry: New opportunities for green chemistry*, World Scientific, 2017, 170 p.
  7. M. Draye, J. Estager and N. Kardos, In: *Activation Methods: Sonochemistry and High Pressure*, (Eds J.-P. Goddard, M. Malacria and C. Ollivier), Willey, 2019, 26.
  8. B. G. Pollet, *Electrocatal.* 2014, **5**, 330.
  9. N. Ghasemi, F. Zare, P. Davari, P. Weber, C. Lagton and A. Gosh, *Proceedings of the 7th IEEE Conference on Industrial Electronics and Applications (ICIEA)*, 2012, 647.
  10. B. Fay and M. Rinker, *Ultrason.*, 1996, **34**, 563.
  11. L. He, F. Zhu, Y. Chen, K. Duan, X. Lin, Y. Pan and J. Tao, *Rev. Sci. Instrum.*, 2016, **87**, 054903.
  12. G. Harris, *Ultras. Med. Biol.*, 1985, **11**, 803.
  13. T. Uchida, T. Kikuchi, M. Yoshioka, Y. Matsuda and R. Horiuchi, *Acoust. Sci. Tech.*, 2015, **36**, 445.
  14. N. Navarro, T. Chave, P. Pochon, Il. Bisel, and S. Nikitenko, *J. Phys. Chem. B*, 2011, **115**, 2024.
  15. I. Margulis and M. Margulis, *Acoust. Phys.*, 2005, **51**, 695.
  16. C. C. Church, D. F. Gaitan, Y. A. Pishchalnikov and T. J. Matula, *J. Acoust. Soc. Am.*, 2011, **129**, 2620.
  17. H. Delmas, N. Tuan Le, L. Barthe and C. Julcour-Lebigue, *Ultrason. Sonochem.*, 2015, **25**, 51.

- 
18. Y. T. Shah, A. B. Pandit and V. S. Moholkar, In: *Cavitation Reaction Engineering*, The Plenum Chemical Engineering Series, Dan Luss Editor, Springer Science, 1999, 79.
19. J. Rooz, E. V. Rebrov, J. C. Schouten and J. T.F. Keurentjes, *Ultrason. Sonochem.* 2013, **20**,1.
20. B. E. Noltingk and E. A. Neppiras, *Proc. Phys. Soc. B* 1950, **63**, 674.
21. L. H. Thompson and L. K. Doraiswamy, *Ind. Eng. Chem. Res.* 1999, **38**, 1215.
22. T. J. Mason and J. P. Lorimer, *Applied sonochemistry: the uses of power ultrasound in chemistry and processing.* 2002.
23. G. Cravotto and P. Cintas, *Chem. Soc. Rev.*, 2006, **35**, 180.
- 24 P. R. Gogate, P. N. Patil, *Sonochemical reactors*, In: *Sonochemistry*, Springer, 2017, 255.
- 25 V. S. Moholkar, S. P. Sable and A. B. Pandit, *AIChE J.* 2000, **46**, 684.
- 26 J.-P. Bazureau and M. Draye, *Ultrasound and Microwaves: Recent Advances in Organic Chemistry*, Transworld Research Network, Kerala, 2011, 241.
- 27 G. Chatel, M. Draye, R. Duwald, C. Piot and P. Fanget, Patent FR 20 06171, 2020.
- 28 Y. Iida, K. Yasui, T. Tuziuti and M. Sivakumar, *Microchem. J.*, 2005, **80**, 159.
- 29 Y. Asakura, M. Maebayashi, T. Matsuoka and S. Koda, *Electron. Commun. Japan*, 2007, **90**, 1.
- 30 K. Makino, M. M. Mossoba, and P. Riesz, *J. Amer. Chem. Soc.*, 1982, **104**, 3537.

- 
- 31 E. N. Harvey, *J. Amer. Chem. Soc.*, 1939, **61**, 2392.
- 32 Y. Hu, Z. Zhang and C. Yang, *Ultrason. Sonochem.*, 2008, **15**, 665.
- 33 R. J. Wood, J., Lee and M. J. Bussemaker, *Ultrasonics Sonochem.*, 2019, **58**, 104645.
- 34 Q.-A. Zhang, Y. Shen, X.-H. Fan, J. F. Garcia Martin, X. Wang and Y. Song, *Ultrason. Sonochem.* 2015, **27**, 96.
- 35 W. B. McNamara, Y. Didenko and K. S. Suslick, *Nature*, 1999, **401**, 772.
- 36 K. Yasuda, T. Torii, K. Yasui, Y. Iiad, T. Tuziuti, M. Nakamura and Y. Asakura, *Ultrason. Sonochem.* 2007, **14**, 699.
- 37 G. Chatel, *Ultrason. Sonochem.*, 2018, **40**, 117.
- 38 G. Cravotto, E. Borretto, M. Oliverio, A. Procopio and A. Penoni, *Catal. Commun.*, 2015, **63**, 2.
- 39 A. Tuulmets, S. Salmar and J. Järv, *Sonochemistry in water organic solutions*, Novinka Books, 2010, 54 p.
- 40 T. Lepoint and F. Lepoint-Mullie, In: *Synthetic Organic Sonochemistry*, ed. J.-L. Luche, Springer, Boston, MA, 1998.
- 41 G. H. Mahdavinia, S. Rostamizadeh, A. M. Amani and Z. Emdadi, *Ultrason. Sonochem.*, 2009, **16**, 7.
- 42 T. Deligeorgiev, S. Kaloyanova, N. Lesev and J. J. Vaquero, *Ultrason. Sonochem.*, 2010, **17**, 783.
- 43 A. Maleki, *Ultrason. Sonochem.*, 2018, **40**, 460.

---

44 I. Mohammadpoor-Baltork, M. Moghadam, S. Tangestaninejad, V. Mirkhani and Z. Eskandari, *Ultras. Sonochem.*, 2010, **17**, 857.

45 R. S. Disselkamp, Y.-H. Chin and C. H. F. Peden, *J. Catal.*, 2004, **227**, 552.

46 P. Qiu, B. Park, J. Choi, B. Thokchom, A. B. Pandit and J. Khim, *Ultras. Sonochem.*, 2018, **45**, 29.

47 N. Bremond, M. Arora, S. M. Dammer and D. Lohse, *Phys. Fluids*, 2006, **18**, 121505.

48 D. E. Yount, E. W. Gillary and D. C. Hoffman, *J. Acous. Soc. Amer.*, 1984, **76**, 1511.

49 P. Gholami, A. Khataee, R. D. C. Soltani and A. Bhatnagar, *Ultras. Sonochem.*, 2019, **58**, 104681.

50 Z. S. Kinzyabaeva and G. L. Sharipov, *Ultras. Sonochem.*, 2018, **42**, 119.

51 T. Ando, S. Sumi, T. Kawate, J. Ichihara and T. Hanafusa, *J. Chem. Soc., Chem. Commun.*, 1984, 439.

52 J.-L. Luche, *Ultras. Sonochem.*, 1996, **3**, S215.

53 U. Neuenschwander, J. Neuenschwander and I. Hermans, *Ultrason. Sonochem.*, 2012, **19**, 1011.

54 R. Naik, A. Nizam, A. Siddekha and M. A Pasha, *Ultrason. Sonochem.*, 2011, **18**, 1124.

55 P. N. Amaniampong, A. Karam, Q. T. Trinh, K. Xu, H. Hirao, F. Jérôme and G. Chatel, *Sci. Rep.*, 2017, **7**, 40650.

- 
- 56 T. Cousin, G. Chatel, N. Kardos, B. Andrioletti and M. Draye, *Ultrason. Sonochem.*, 2019, **53**, 120.
- 57 P. Hu, Y. Ben-David and D. Milstein, *J. Am. Chem. Soc.*, 2016, **138**, 6143.
- 58 P. Contant, L. Forzy, U. Hengartner and G. Moine, *Helv. Chim. Acta*, 1990, **73**, 1300.
- 59 W. Lijinsky, *Cancer Res.* 1974, **34**, 255.
- 60 D. Lambert, *Local Anesthetic Pharmacology*, In: Stanley T.H., Ashburn M.A. (eds) *Anesthesiology and Pain Management. Developments in Critical Care Medicine and Anesthesiology*, Springer, 1994, Vol 29, 35.
- 61 S. Perrin, D. Montani, C. O'Connell, S. Günther, B. Girerd, L. Savale, C. Guignabert, O. Sitbon, G. Simonneau, M. Humbert and M.-C. Chaumais, *Eur. Respir. J.*, 2015, **46**, 1211.
- 62 R. Rothman and M. Baumann, *Eur. J. Pharmacol.*, 2003, **479**, 23.
- 63 L. Antkiewicz-Michaluk, I. Romanska, A. Wąsik and J. Michaluk, *Neurotox. Res.*, 2017, **32**, 94.
- 64 T. Kahl, K.-W. Schröder, F. Lawrence, W. Marshall, H. Höke and R. Jäckh, *Aniline*, In: *Ullmann's Encyclopedia of Industrial Chemistry*, Ed. Wiley-VCH, 2012.
- 65 S. M. Kelly and B. H. Lipshutz, *Org. Lett.*, 2014, **16**, 98.
- 66 M. Draye, G. Chatel and R. Duwald, *Pharmaceuticals*, 2020, **13**, 1.
- 67 M. K. Basu, F. F. Becker and B. K. Banik, *Tetrahedron Lett.*, 2000, **41**, 5603.

- 
- 68 O. Elendu, M. Ojewumi, Y. D. Yeboah and E. E. Kalu, *Int. J. Electrochem. Sci.*, 2015, **10**, 10792.
- 69 ECHA, Sodium phosphinate, online: <https://echa.europa.eu/fr/substance-information/-/substanceinfo/100.028.791> (accessed December 2020).
- 70 S. Letort, M. Lejeune, N. Kardos, E. Métay, F. Popowycz, M. Lemaire and M. Draye, *Green Chem.*, **2017**, 19, 4583.
- 71 G. Chen, Z. Liu, Y. Zhang, X. Shan, L. Jiang, Y. Zhao, W. He, Z. Feng, S. Yang and G. Liang, *ACS Med. Chem. Lett.*, 2013, **4**, 69.
- 72 M. Gaba, S. Singh and C. Mohan, *Eur. J. Med. Chem.*, 2014, **76**, 494.
- 73 N. Nongrum, G. K. Kharmawlong, J. W. S. Rani, N. Rahman, A. Dutta and R. Nongkhlaw, *J. Heterocycl. Chem.*, 2019, **56**, 2873.
- 74 S. Sarhandi, L. Zare Fekri and E. Vessally, *Acta Chim. Slov.*, 2018, **65**, 246.
- 75 M. Mohamed, *J. Pharm. Sci.*, 2016, **53**, 108.
- 76 B. H. Han and P. Boudjouk, *J. Org. Chem.*, 1982, **47**, 5030.
- 77 P. Boudjouk, D. P. Thompson, W. H. Ohrbom and B. Han, *Organometallics*, 1986, **5**, 1257.
- 78 K. S. Suslick and S. J. Doktycz, *J. Am. Chem. Soc.*, 1989, **111**, 2342.
- 79 N. A. Ross and R. A. Bartsch, *J. Heterocycl. Chem.*, 2001, **38**, 1255.
- 80 N. A. Ross and R. A. Bartsch, *J. Org. Chem.* 2003, **68**, 360.
- 81 R. G. Soengas and A. M. Estévez, *Ultrason. Sonochem.*, 2012, **19**, 916.
- 82 C.-J. Li, *Tetrahedron*, 1996, **52**, 5643.

- 
83. S. M. Cenci, L. R. Cox and G. A. Leeke, *ACS Sustainable Chem. Eng.* 2014, **2**, 1280.
84. B. D. Mather, K. Viswanathan and K. M. Miller, T. E. Long, *Prog. Polym. Sci.* 2006, **31**, 487.
85. J. Christoffers, *Eur. J. Org. Chem.* 1998, **1998**, 1259.
86. Y.-L. Song, Y.-F. Dong, F. Wu, T. Yang and G.-L. Yang, *Ultrason. Sonochem.*, 2015, **22**, 119.
87. A. Koleva, N. Petkova and R. Nikolova, *Synlett*, 2016, **27**, 2676.
88. B. Banerjee, *Ultrason. Sonochem.* 2017, **35**, 1.
89. M. Draye and N. Kardos, *Top. Curr. Chem.*, 2016, **374**, 74.
90. P. R. Gogate, V. S. Sutkar and A. B. Pandit, *Chem. Eng. J.*, 2011, **166**, 1066.
91. V. S. Sutkar and P. R. Gogate, *Chem. Eng. J.*, 2009, **155**, 26.
92. J. W. K. Kambiz Farahmand, *Exp. Heat Transfer*, 2001, **14**, 107.
93. Y. Iida, K. Yasui, T. Tuziuti and M. Sivakumar, *Microchem. J.*, 2005, **80**, 159.
94. S. Merouani, O. Hamdaoui, Y. Rezgui and M. Guemini, *Res. Chem. Intermediat.*, 2015, **41**, 881.
95. K. Yasui, T. Kozuka, T. Tuziuti, A. Towata, Y. Iida, J. King and P. Macey, *Ultrason Sonochem.*, 2007, **14**, 605.
96. N. Kerabchi, S. Merouani and O. Hamdaoui, *Ultrason. Sonochem.*, 2018, **48**, 136.

- 
97. N. Kerabchi, S. Merouani and O. Hamdaoui, *Separ. Purif. Technol.*, 2018, **206**, 118.
98. Y. T. Didenko and K. S. Suslick, *Nature*, 2002, **418**, 394.
99. S. Koda, K. Tanaka, H. Sakamoto, T. Matsuoka and H. Nomura, *J. Phys. Chem.*, 2004, **108**, 11609.
100. A. A. Doinikov and S. T. Zavtrak, *Physics Fluids*, 1995, **7**, 1923.
101. T. Tuziuti, K. Yasui, Y. Iida, M. Sivakumar and S. Koda, *J. Phys. Chem.*, 2004, **108**, 9011.
102. R. A. Sheldon, *Green Chem.* 2007, **9**, 1273.
103. R. A. Sheldon, *ACS Sustainable Chem. Eng.*, 2018, **6**, 32.
104. P. Tierce, Patent, 1998, FR2768948B1, WO1999016558A1.
105. S. I. Nikitenko, M. Brau, R. Pflieger, *Ultrason. Sonochem.*, 2020, **67**, 105189.
106. C. Cau, Y. Guari, T. Chave, J. Larionova, P. Pochon and S. I. Nikitenko, *J. Phys. Chem.*, 2013, **117**, 22827.
107. S. Balachandran, S. E. Kentish, R. Mawson and M. Ashokkumar, *Ultrason. Sonochem.*, 2006, **13**, 471.
108. E. S. Dasso and Y. O. Li, *Trends Food Sci. Technol.*, 2019, **86**, 492.
109. G. Cravotto and P. Cintas, *Chem. Eur. J.*, 2007, **13**, 1902.
110. V. G. Gude, *Resource-Efficient Technologies*, 2015, **1**, 116.
111. Y. Peng and G. Song, *Green Chem.*, 2003, **5**, 704.

- 
112. D. Fernandez Rivas and S. Kuhn, *Top. Curr. Chem.*, 2016, **374**, 70.
113. J. Sedelmeier, S. V. Ley, I. R. Baxendale and M. Baumann, *Org. Lett.*, 2010, **12**, 3618.
114. C. Delacour, D. Stephens, C. Lutz, R. Mettin and S. Kuhn, *Org. Process Res. Dev.*, 2020, **24**, 2085.
115. Y. Naruke, H. Tanaka and H. Harada, *Electrochemistry*, 2011, **79**, 826.
116. G. Chatel and D. R. MacFarlane, *Chem. Soc. Rev.*, 2014, **43**, 8132.
117. G. Kaur, A. Sharma and B. Banerjee, *ChemistrySelect*, 2018, **3**, 5283.
118. G. Chatel, R. Pflieger, E. Naffrechoux, S. I. Nikitenko, J. Suptil, C. Goux-Henry, N. Kardos, B. Andrioletti and M. Draye, *ACS Sustainable Chem. Eng.*, 2013, **1**, 137.
119. N. D. Oktavianti, Kartinin and A. Mun'im, *Heliyon*, 2019, **5**, e02950.
120. D. Panda and S. Manickam, *Ultrason. Sonochem.*, 2017, **36**, 481.
121. Y. Son, M. Lim, J. Khim and M. Ashokkumar, *Ind. Eng. Chem. Res.*, 2012, **51**, 232.
122. R. Abazari, A. R. Mahjoub, S. Sanati, Z. Rezvani, Z. Hou and H. Dai, *Inorg. Chem.*, 2019, **58**, 1834.
123. S. Saito, *Ultrasound Field and Bubbles*, In: *Sonochemistry and the Acoustic Bubble*, Elsevier Inc., 2015, 11.